CELL CYCLE

Role of protein kinase PLK1 in the epigenetic maintenance of centromeres

Duccio Conti[1]*, Arianna Esposito Verza[1,2], Marion E. Pesenti[1], Verena Cmentowski[1,2], Ingrid R. Vetter[1], Dongqing Pan[1]†, Andrea Musacchio[1,2]*

The centromere, a chromosome locus defined by the histone H3–like protein centromeric protein A (CENP-A), promotes assembly of the kinetochore to bind microtubules during cell division. Centromere maintenance requires CENP-A to be actively replenished by dedicated protein machinery in the early G_1 phase of the cell cycle to compensate for its dilution after DNA replication. Cyclin-dependent kinases (CDKs) limit CENP-A deposition to once per cell cycle and function as negative regulators outside of early G_1. Antithetically, Polo-like kinase 1 (PLK1) promotes CENP-A deposition in early G_1, but the molecular details of this process are still unknown. We reveal here a phosphorylation network that recruits PLK1 to the deposition machinery to control a conformational switch required for licensing the CENP-A deposition reaction. Our findings clarify how PLK1 contributes to the epigenetic maintenance of centromeres.

During cell division, kinetochores enable the segregation of sister chromatids by mediating their interaction with the mitotic spindle (*1*). Kinetochores form at specialized chromatin loci called centromeres (*2*–*6*). The maintenance of centromeres' position along the chromosome axis is of utmost importance for cell viability (*7*). With few exceptions, the specialized histone centromeric protein A (CENP-A) defines the location of centromeres, functioning as an epigenetic marker (*8*–*10*). In higher eukaryotes, CENP-A dynamics on chromatin differ from those of canonical H3.1 histones, which are incorporated during DNA replication (*11*, *12*). CENP-A replenishment in telophase or early G_1 phase compensates for its dilution during S phase (*13*, *14*) (Fig. 1A). A dedicated group of conserved proteins, collectively called the CENP-A deposition machinery, orchestrates this event. Specifically, Holliday junction recognition protein (HJURP), a CENP-A–specific chaperone, stabilizes the cytosolic form of CENP-A (*15*, *16*). Targeting HJURP to centromeres requires the octameric missegregation protein 18 (MIS18) complex, composed of two MIS18 binding protein 1 ($M18BP1^{hKNL2}$) subunits, four MIS18α subunits, and two MIS18β subunits (*17*–*22*). The hierarchical interaction of HJURP with the MIS18 complex is essential for centromere inheritance (*23*, *24*). Finally, the mechanism of new CENP-A incorporation likely requires a source of energy, as was demonstrated for other histone variants (*25*). Several chromatin remodelers have been reported to interact with kinetochore proteins (*26*–*31*), but their precise function at centromeres remains obscure.

The CENP-A deposition process echoes the regulatory network that limits the initiation of DNA replication to only once per cell cycle. In the case of CENP-A, the process is licensed at mitotic exit and early G_1 phase by the deactivation of cyclin-dependent kinases (CDKs), which act as potent inhibitors of CENP-A deposition in all of the other cell cycle phases. CDKs phosphorylate a constellation of residues across the CENP-A deposition machinery, preventing its untimely assembly (Fig. 1, B and C). Specifically, CDKs negatively regulate CENP-A:HJURP recruitment to centromeres (*32*), repress the interaction of HJURP with the MIS18 complex, and prevent M18BP1 binding to MIS18αβ, which in turn blocks their centromere localization (*17*, *19*, *33*, *34*). Adding another layer of complexity to this network, Polo-like kinase 1 (PLK1) activity is essential for new CENP-A deposition (*35*). Thus, two kinases with opposing functions control the epigenetic maintenance of centromeres, but how PLK1 regulates this process remains unknown (Fig. 1C). In this study, we elucidate this fundamental molecular mechanism, decoding it from the multiplicity of other functions that PLK1 performs during mitotic exit (*36*–*39*). We show that PLK1 activity is essential to controlling a conformational switch of the MIS18α's N-terminal region that licenses the recruitment of HJURP to centromeres. PLK1 binds sequentially to M18BP1, MIS18α, and HJURP, and its physical interaction is required to promote CENP-A deposition, thus defining PLK1 as an integral part of the deposition machinery.

M18BP1 is the apical regulator of PLK1 recruitment to centromeres during early G_1 phase

PLK1 activity during mitotic exit possibly regulates the recruitment of the deposition machinery to centromeres (*35*). Inhibition of both CDK1 and PLK1 did not rescue the requirement for PLK1 activity in this process (*35*) (figs. S1 and S2), indicating that the defects in CENP-A deposition are not caused by ectopic CDK1 activity upon inactivation of PLK1. To disentangle the role of PLK1 in this pathway from its other essential functions during mitotic exit, we examined its recruitment mode to centromeres in early G_1, which depends on M18BP1 and MIS18αβ, but not HJURP (*35*) (fig. S3). The first 490 residues of M18BP1 contain the determinants of centromere recognition of the deposition machinery (*35*), suggesting that PLK1-binding sites might also occur in this fragment. To investigate this, we incubated recombinant $M18BP1^{1\text{-}490}$ with the Polo-box domain (PBD) of PLK1, a specific phospho–amino acidic adapter that promotes the docking of PLK1 to previously phosphorylated motifs (*40*). Substoichiometric amounts of full-length PLK1 were added to trigger phosphorylation. This strategy allowed us to use the PBD at concentrations similar to those of $M18BP1^{1\text{-}490}$ but in the presence of limiting kinase activity to promote specific phosphorylation (*39*). We also added to the mixture substoichiometric amounts of CDK1, which primes PLK1 binding to various substrates during mitosis, including the kinetochore (*41*). We then examined the complex assembly between $M18BP1^{1\text{-}490}$ and the PBD in solid phase. PLK1 interacted with a region spanning M18BP1's first 140 residues (fig. S4A). Detailed analysis of this domain identified Thr78 and Ser93 as highly conserved residues that might participate in the interaction (Fig. 1D). Antibodies raised against the phosphorylated versions of these two residues showed that Thr78 is a PLK1-specific substrate, whereas Ser93 can be phosphorylated by both PLK1 and CDK1 in vitro (fig. S4, B and C). We used analytical size-exclusion chromatography (SEC) to assess the relative contributions of these kinases in triggering PLK1 binding to M18BP1. Phosphorylation by PLK1, but not by CDK1, was sufficient for a stoichiometric interaction of the PBD with $M18BP1^{1\text{-}490}$ (fig. S5). Mutating both Thr78 and Ser93 abolished the interaction between $M18BP1^{1\text{-}490}$ and PBD in vitro, whereas the single mutations weakened it (Fig. 1E). We used rescue assays to study the extent of PLK1 recruitment to centromeres in human cells. In these experiments, depletion of the endogenous M18BP1 is compensated by the expression of an inducible small interfering RNA–resistant, fluorescently tagged M18BP1. For each rescue assay in this work, we assessed in parallel the efficiency of depletion in the parental cells. Individually mutating Thr78 or Ser93 was sufficient to abrogate the recruitment of PLK1 to centromeres in early G_1 (Fig. 1, F and G, and fig. S6). Residual binding of the single mutants in vitro likely reflects the higher protein concentrations of binding species used

[1]Department of Mechanistic Cell Biology, Max Planck Institute of Molecular Physiology, 44227 Dortmund, Germany. [2]Centre for Medical Biotechnology, Faculty of Biology, University of Duisburg-Essen, 45141 Essen, Germany.
*Corresponding author. Email: andrea.musacchio@mpi-dortmund.mpg.de (A.M.); duccio.conti@mpi-dortmund.mpg.de (D.C.)
†Present address: Research Division, Chugai Pharmaceutical Co., Ltd., Yokohama 244-8602, Japan.

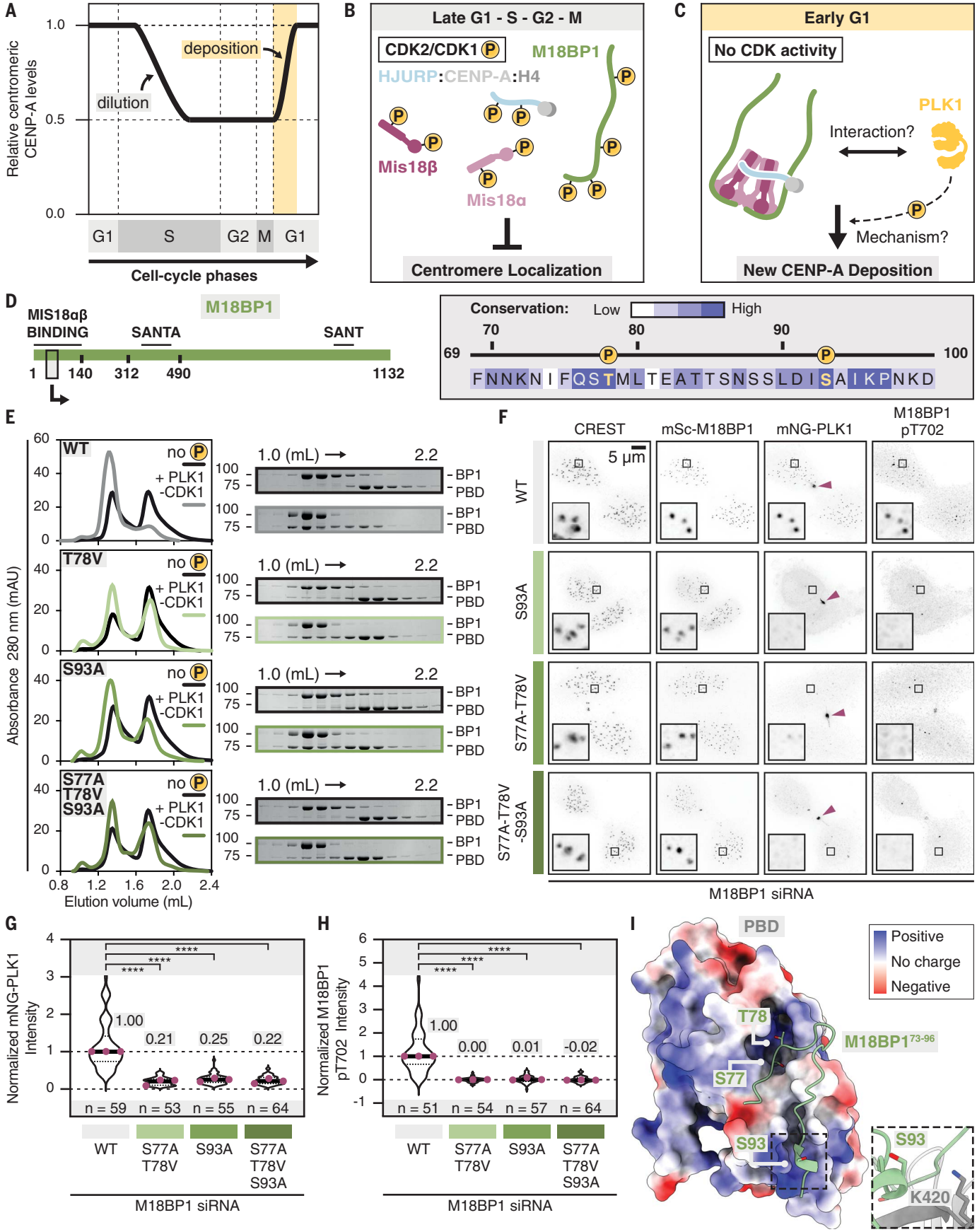

Fig. 1.

Fig. 1. M18BP1 is the apical regulator of PLK1 recruitment to centromeres in early G_1. (**A**) Chromatin-bound CENP-A gets halved during DNA replication and replenished to its initial level in early G_1 phase. (**B**) CDK kinases negatively regulate the assembly of the complete CENP-A deposition machinery and prevent its centromeric localization during the late G_1, S, and G_2 phases and mitosis. (**C**) During early G_1 phase, reduced CDK activity allows the CENP-A deposition machinery to localize to centromeres. PLK1 activity is also needed to license the mechanism. (**D**) Diagram showing the location of the PLK1-binding site on M18BP1. The inset displays the evolutionary conservation of the domain. (**E**) Analytical SEC of MBP-M18BP1$^{1\text{-}490}$ (WT or mutants) incubated with MBP-PBD in the presence or absence of kinase activity. (**F**) Centromeric localization of mNeonGreen-PLK1 and enrichment of M18BP1 pThr702 signal in human cells expressing mScarlet-M18BP1 (WT or mutants) in early G_1 phase. Arrowheads indicate the position of the spindle midbody. (**G**) Quantification of mNeonGreen-PLK1 intensity from cells in (F). (**H**) Quantification of M18BP1 pThr702 intensity from cells in (F). Magenta dots show the median value of each experimental repeat. (**I**) AlphaFold2 model showing the docking of M18BP1's Ser77 and Thr78 to the canonical binding pocket of PBD. Ser93 is predicted to interact with a proximal positively charged patch (highlighted in the inset).

in these assays (in the micromolar range) relative to those in the cellular environment (estimated in the low-nanomolar range). Cells expressing the M18BP1 phosphorylation mutants retained normal cytokinesis and PLK1 localization at the spindle midbody remnant but had decreased PLK1 localization and centromere activity, as measured by visualizing M18BP1's Thr702, a known PLK1 substrate (*35*) (Fig. 1, F and H).

SEC coupled with multiangle light-scattering measurements demonstrated that M18BP1 and PLK1 bind in a 1:1 stoichiometry (fig. S7, A and B), suggesting that the two closely spaced phosphorylation sites dock on a single PLK1 molecule. AlphaFold2 (*42*) predicts that Thr78, which is part of a canonical PBD-binding motif (S-S,T-X), docks into the canonical phosphosite-binding pocket of PLK1's PBD, whereas Ser93 engages a nearby positively charged patch, thus strengthening the interaction upon phosphorylation (Fig. 1I and fig. S7C). These results show that M18BP1 is the apical regulator of PLK1 recruitment to centromeres during early G_1 phase.

Centromeric PLK1 is required for HJURP recruitment to centromeres in early G_1

Given that PLK1 recruitment in early G_1 is lost in the M18BP1 point mutants, we studied the effects of such mutations on the localization of the deposition machinery and CENP-A deposition. In rescue assays, M18BP1 point mutants failed to load new CENP-A at centromeres (Fig. 2, A and B, and fig. S8, A and B). Ablation of PLK1 recruitment by the mutations had little or no effect on the centromeric localization of M18BP1 and MIS18α, a proxy for the MIS18αβ complex (Fig. 2A and fig. S8, C and D). M18BP1's binding region to MIS18αβ (residues 1 to 140) encompasses the PLK1-binding site, but mutations at Thr78 and Ser93 did not affect the binding to the MIS18αβ complex in an analytical SEC experiment (fig. S9). These results imply that PLK1 regulates a process downstream from the assembly of the MIS18 complex. Using M18BP1$^{S77A\text{-}T78V\text{-}S93A}$ as the representative PLK1 loss-of-binding mutant, we examined HJURP recruitment using the same strategy as above. Expressing M18BP1$^{S77A\text{-}T78V\text{-}S93A}$ in cells resulted in an almost complete loss of HJURP from centromeres (Fig. 2, C and D, and fig. S10). We conclude that, during early G_1, PLK1 binds to the N-terminal region of M18BP1 and positively regulates HJURP recruitment to centromeres to promote new CENP-A deposition (Fig. 2E).

PLK1 relieves MIS18α's N terminus negative regulation of HJURP recruitment to centromeres

A region encompassing the N-terminal 55 residues of MIS18α exerts an inhibitory effect in vitro on the interaction of HJURP with the MIS18αβ complex (*23*), possibly reflecting a conformational switch. We surmised that PLK1 phosphorylation might regulate this activity. We tested this hypothesis in an in vitro reconstitution system consisting of the MIS18αβ complex and the C-terminal region of HJURP encompassing the R2 repeat (541-C fragment), which binds MIS18αβ (*23*). We performed the experiment at concentrations that allowed us to detect the possible changes in binding affinity resulting from PLK1 activity. Phosphorylation by PLK1 alone was insufficient for complex formation (Fig. 3A, black trace, and fig. S11A). We then added the PBD at concentrations expected to saturate all the possible docking sites to mimic PLK1 binding. Under these conditions, a stable complex composed of HJURP$^{541\text{-}C}$, MIS18αβ, and PBD formed (Fig. 3A, cyan trace). Complex formation was dependent on PLK1 activity (Fig. 3A, compare gray and cyan traces). This complex incorporated all of the components above, because mixing MIS18αβ (the largest constituent) and PBD without HJURP resulted in a smaller complex (Fig. 3A, compare cyan and green traces). Performing the same experiment with HJURP R1 repeat (394 to 540 fragment), which also binds the MIS18αβ complex, yielded a similar outcome (fig. S11, B and C). Further study of this mechanism showed that PLK1 interacts with a conserved motif enclosed in MIS18α's first 55 residues, and that binding was dependent on the phosphorylation of Ser54 of MIS18α (Fig. 3B and fig. S12). These results show that PLK1, contingent on phosphorylation of and binding to MIS18α, relieves a steric blockade of MIS18α's N-terminal region on the HJURP-binding site, thus promoting the formation of the HJURP:MIS18αβ complex.

PLK1 binds to both MIS18α and HJURP to license new CENP-A deposition

Our exploration of the docking of PLK1 on the HJURP:MIS18αβ complex also uncovered a conserved PBD-binding domain in the HJURP C-terminal region, which required phosphorylation of Thr654 (Fig. 3C and fig. S13). Incubating recombinant MIS18α$^{S53A\text{-}S54A}$β with HJURP$^{S653A\text{-}T654V}$ abrogated the formation of the HJURP:MIS18αβ complex in analytical SEC, even in the presence of PBD and PLK1 activity (Fig. 3D). Different combinations of wild-type (WT) and mutant proteins resulted in complexes exhibiting intermediate affinities (fig. S14). To demonstrate that the interaction of PLK1 with both MIS18α and HJURP is essential to driving successful CENP-A deposition in a cellular context, we performed rescue assays in which HJURP$^{S653A\text{-}T654V}$ and MIS18α$^{S53A\text{-}S54A}$, both fluorescently labeled, were coexpressed in HeLa cells depleted of the respective endogenous proteins. As predicted, coexpression of the two mutants decreased CENP-A deposition (Fig. 3, E to H, and fig. S15) and reduced the centromeric recruitment of HJURP to levels similar to those exhibited by the M18BP1$^{S77A\text{-}T78V\text{-}S93A}$ mutant (compare Fig. 3, E and G, with Fig. 2, C and D). As anticipated by the binding assays, the expression of individual point mutants of either MIS18α or HJURP in HeLa cells only mildly affected CENP-A deposition (figs. S16 and S17). We conclude that simultaneous binding of PLK1 to MIS18α and HJURP is needed to counteract the negative activity of the MIS18α N terminus and to license successful CENP-A deposition (Fig. 3I).

The role of PLK1 in the epigenetic maintenance of centromeres revolves around the MIS18α conformational switch

PLK1-licensing activity lies in its ability to regulate the conformation of the MIS18α N-terminal region (Fig. 3). If this were the primary role of PLK1 in the pathway of CENP-A deposition, then we speculated that removing MIS18α's inhibitory domain should allow CENP-A deposition in the absence of PLK1 activity at centromeres. To verify this, we designed a rescue assay in human cells in which M18BP1$^{S77A\text{-}T78V\text{-}S93A}$, which prevents PLK1 recruitment to centromeres, was coexpressed with MIS18α$^{56\text{-}C}$ in cells depleted of the endogenous proteins. As shown above, expression of M18BP1$^{S77A\text{-}T78V\text{-}S93A}$ abrogated CENP-A deposition (Fig. 4, A and B, and fig. S18). Cells expressing MIS18α$^{56\text{-}C}$ alongside M18BP1$^{S77A\text{-}T78V\text{-}S93A}$ incorporated new CENP-A to substantial levels (58% efficiency compared

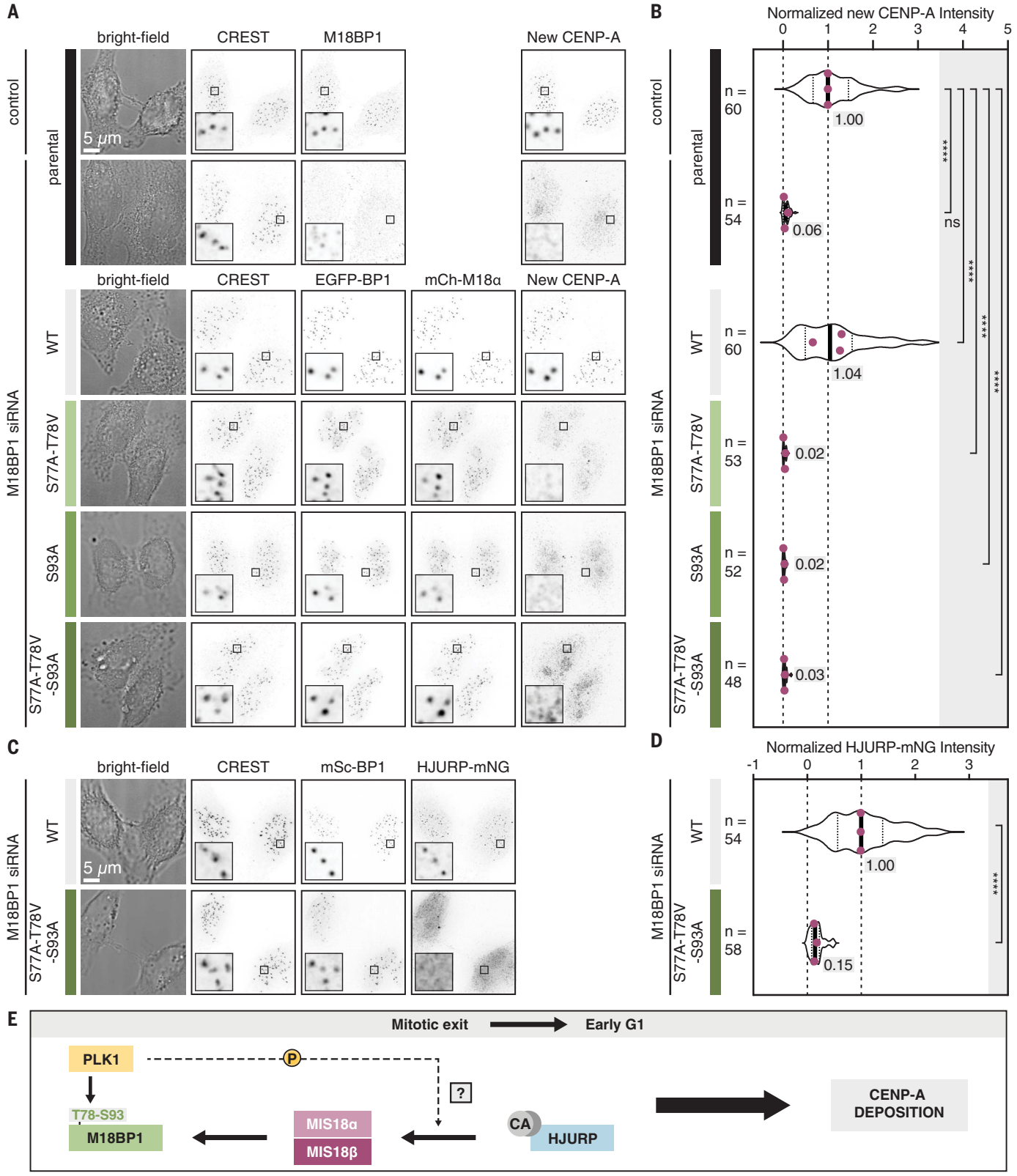

Fig. 2. Centromeric PLK1 is required for HJURP recruitment to centromeres in early G_1. (**A**) EGFP-M18BP1, mCherry-MIS18α, and new CENP-A levels at centromeres in human cells expressing EGFP-M18BP1 (WT or mutants) in early G_1 phase. The top panels show the parental cells as controls for the endogenous M18BP1 depletion. (**B**) Quantification of new CENP-A levels in cells from (A). Magenta dots show the median value of each experimental repeat. (**C**) HJURP-mNG levels in human cells expressing M18BP1 (WT or S77A-T78V-S93A mutant) in early G_1 phase. (**D**) Quantification of HJURP-mNG intensity in cells from (C). Magenta dots show the median value of each experimental repeat. (**E**) Summary diagram. In early G_1, PLK1 binds to M18BP1's N terminus and regulates HJURP localization to centromeres to allow CENP-A deposition. CA, CENP-A.

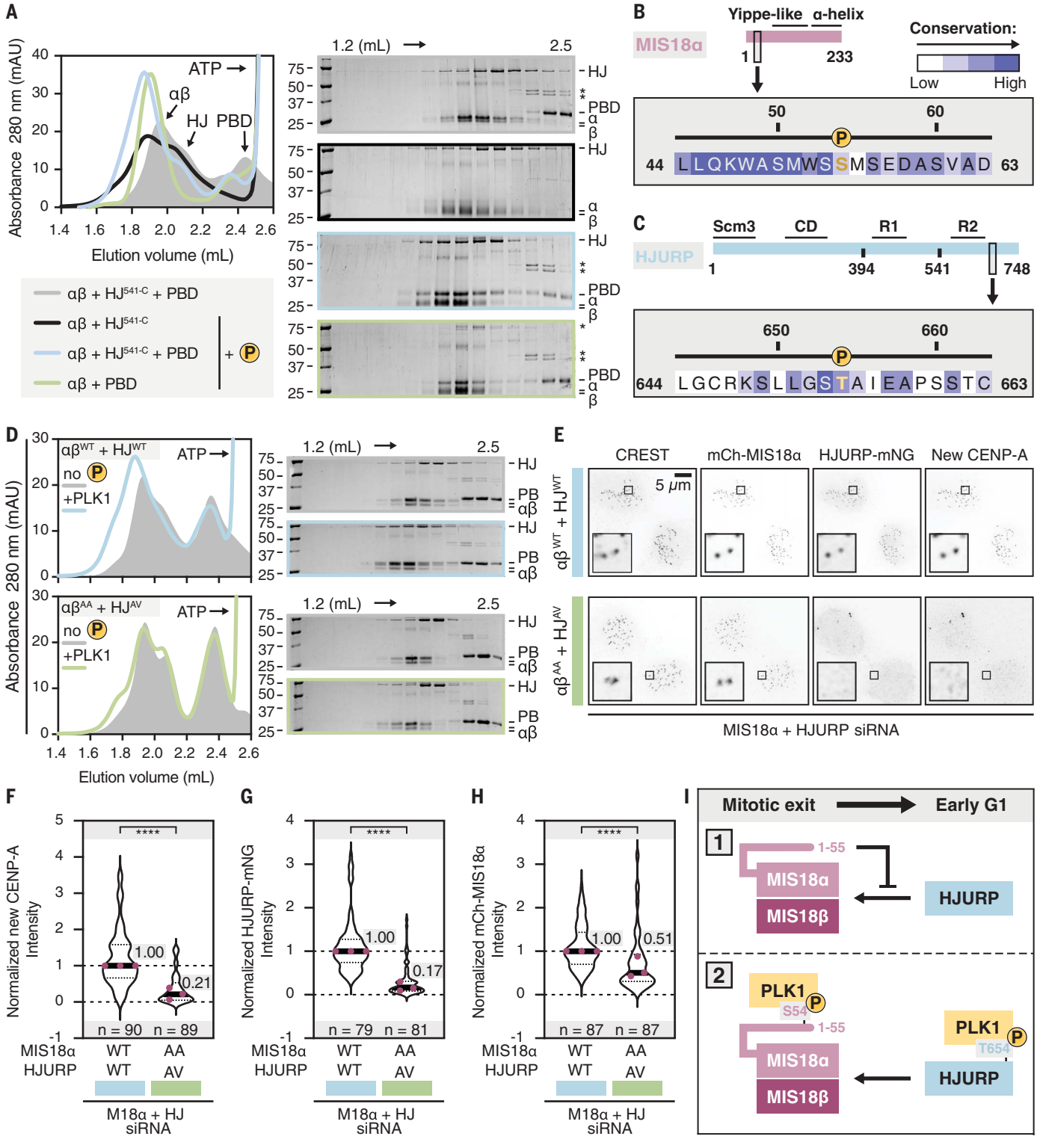

Fig. 3. PLK1 relieves MIS18α's N terminus negative regulation on HJURP recruitment to centromeres. (**A**) Analytical SEC showing that MIS18αβ and HJURP$^{541\text{-}C}$ can bind in the presence of PBD and PLK1 phosphorylation. (**B** and **C**) Diagrams showing the location of the PLK1-binding site on MIS18α and HJURP, respectively. The inset displays the evolutionary conservation of the domain. (**D**) Analytical SEC showing that the HJURP$^{541\text{-}C}$ interaction with MIS18αβ is abrogated when the PBD is not able to bind to both of them. (**E**) mCherry-MIS18α, HJURP-mNG, and new CENP-A levels in human cells coexpressing mCherry-MIS18α and HJURP-mNG (both WT and mutant) in early G_1 phase. (**F**) Quantification of new CENP-A intensity from (E). (**G**) Quantification of HJURP-mNG intensity from (E). (**H**) Quantification of mCherry-MIS18α intensity from (F). Magenta dots show the median value of each experimental repeat. (**I**) Summary diagram. PLK1 phosphorylation of and binding to MIS18α and HJURP enables their interaction by counteracting MIS18α's N terminus negative regulation.

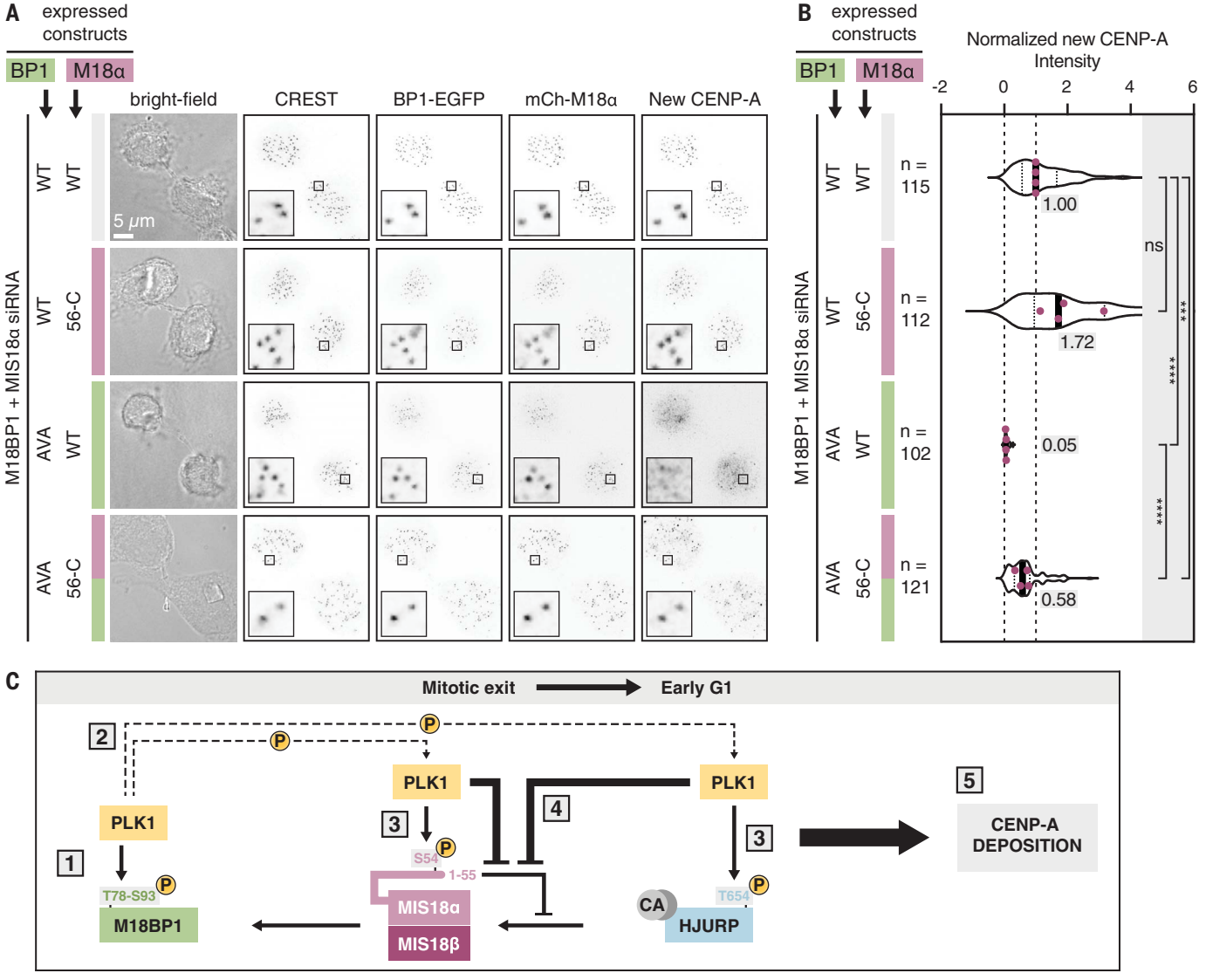

Fig. 4. Role of PLK1 in the epigenetic maintenance of centromeres revolves around MIS18α's conformational switch. (**A**) EGFP-M18BP1, mCherry-MIS18α, and new CENP-A levels in human cells coexpressing EGFP-M18BP1 and mCherry-MIS18α (WT or mutants, expressed in different combinations) in early G_1 cells. (**B**) Quantification of new CENP-A intensity from (A). Magenta dots show the median value of each experimental repeat. (**C**) Summary diagram showing the final model of this study.

with the WT control). Altogether, these results demonstrate that PLK1 promotes CENP-A deposition through the regulation of the MIS18α conformational switch.

PLK1 binding to the CENP-A deposition machinery is hierarchical

Our work shows that PLK1 regulates CENP-A deposition through multiple interactions with the components of the deposition machinery. Because mutating the PLK1-docking site on M18BP1 was sufficient to prevent HJURP localization to centromeres (Fig. 1), it appears that recruitment of the various components of the deposition machinery requires a defined binding hierarchy (*15*, *18*). To test this idea, we investigated whether the PLK1-docking site of M18BP1, which is highly conserved (compare Fig. 1D and Fig. 3, B and C), could sustain CENP-A deposition when grafted onto HJURP. A minimal PLK1-binding fragment of M18BP1 encompassing residues 56 to 98, which bound to PLK1 robustly in analytical SEC experiments (fig. S19), was grafted onto HJURP to replace the PBD-binding motif centered at Thr654 (henceforth called "HJURP^{graft}"; fig. S20A). We coexpressed this mutant with M18BP1$^{S77A\text{-}T78V\text{-}S93A}$, which blocks PLK1 recruitment to centromeres, in HeLa cells depleted of endogenous M18BP1 and HJURP (fig. S20B). The HJURP^{graft} construct did not localize to centromeres and did not allow new CENP-A deposition in the presence of the M18BP1$^{S77A\text{-}T78V\text{-}S93A}$ mutant (fig. S20, C to G). Further confirming that PLK1 licensing of new CENP-A deposition must start with its binding to M18BP1, preventing the docking of PLK1 to another component of the deposition machinery downstream of M18BP1 recruitment (MIS18α$^{S53A\text{-}S54A}$ mutant) barely affected the centromere levels of PLK1 (fig. S21). In addition, blocking HJURP from interacting with PLK1 did not significantly alter its localization to centromeres (fig. S17, D and F).

Discussion

Our work clarifies the role of PLK1 in licensing new CENP-A deposition (*35*). In early G_1, PLK1 binds to M18BP1 on a highly conserved binding site generated by the phosphorylation of two nearby residues, Thr78 and Ser93 (Fig. 4C, step 1), both of which have to be phosphorylated for successful recruitment of PLK1 to centromeres. This doubly phosphorylated site interacts with

a single PBD, possibly with a previously undescribed binding mode (*40*, *43*). M18BP1's Ser93 is a substrate of both PLK1 and CDK1 in vitro. Its sequence resembles noncanonical CDK1 sites previously identified in other mitotic substrates (*44*–*46*), but it is also similar to target sites of the acidophilic PLK1 kinase. This promiscuous regulation hints at possible priming of the binding during mitosis, in parallel with other mitotic PLK1-binding proteins (*41*), implying that the phosphorylated site needs to survive dephosphorylation by protein phosphatase 2A (PP2A-B55) during mitotic exit (*47*).

To overcome the pleiotropic effects of PLK1 inhibitors, we focused on specific phosphorylation sites and separation-of-function mutants. This showed that centromere targeting of M18BP1 and the MIS18αβ complex is minimally sensitive to PLK1 activity, but also uncovered a complex cascade of events that ultimately activate CENP-A discharge by the deposition machinery. We propose that once bound to M18BP1, PLK1 primes the simultaneous binding of additional PLK1 molecules to two downstream components of the CENP-A deposition machinery (Fig. 4C, steps 2 and 3). These interactions require the phosphorylation of Ser54 on MIS18α and Thr654 on HJURP. Our results imply that physical binding of PLK1 to the MIS18α's N-terminal α-helix promotes a conformational switch that is essential for increasing the affinity between HJURP and MIS18αβ (*23*) (Fig. 4C, step 4). All of the PLK1-docking sites mapped in this study are close to the regions that the components of the deposition machinery use to interact with each other (*17*, *19*, *23*, *24*) (fig. S22). Thus, CENP-A deposition appears to require full assembly of this complex (Fig. 4C, step 5). By showing that PLK1 is a tightly docked component, our data imply a structural role of PLK1 in the assembly of the complex. The regulation of the MIS18α's N-terminal region is pivotal for HJURP localization to centromeres, and, accordingly, the MIS18α$^{56\text{-}C}$ mutant was able to load CENP-A in the absence of PLK1 at centromeres.

The recruitment of PLK1 onto the CENP-A deposition machinery appears to be sequential. It depends on binding first to M18BP1, which acts as its apical regulator. Confirming this, the PLK1-binding site of M18BP1 cannot be grafted onto HJURP without losing CENP-A deposition activity. The order of PLK1 binding is also consistent with the sequential centromere localization of the CENP-A deposition machinery during the transition from mitotic exit to early G_1 in human cells (*15*, *18*). The loss of CENP-A incorporation exhibited by the M18BP1$^{S77A\text{-}T78V\text{-}S93A}$ mutant was phenocopied only when both MIS18α$^{S53A\text{-}S54A}$ and HURP$^{S653A\text{-}T654V}$ mutants were coexpressed, whereas the single expression of MIS18α$^{S53A\text{-}S54A}$ and HJURP$^{S653A\text{-}T654V}$ mutants only resulted in mild CENP-A deposition phenotypes. The conservation of the PLK1 sites implies that this mechanism also works in other metazoans. Our analysis does not exclude that PLK1, in addition to controlling the incorporation of HJURP in the MIS18 complex, may regulate further downstream steps in the mechanism of new CENP-A incorporation.

Our study provides insight into how cells replenish the centromere epigenetic marker at every cell cycle. This safety mechanism must satisfy two conditions to allow the deposition reaction to take place: CDK1 sites must be dephosphorylated (*17*, *32*–*34*) and PLK1 must phosphorylate and bind to M18BP1, MIS18α, and HJURP (*35*). This elegant solution harnessing the action of CDK1 and PLK1, two kinases with opposite functions, restricts the deposition reaction to the early G_1 phase. Our findings are consistent with and complementary to the work of Parashara *et al.* (*48*).

REFERENCES AND NOTES

1. A. Musacchio, A. Desai, *Biology* **6**, 5 (2017).
2. E. Zasadzińska, D. R. Foltz, *Prog. Mol. Subcell. Biol.* **56**, 165–192 (2017).
3. T. Fukagawa, W. C. Earnshaw, *Dev. Cell* **30**, 496–508 (2014).
4. J. Ohzeki, V. Larionov, W. C. Earnshaw, H. Masumoto, *Curr. Opin. Cell Biol.* **58**, 15–25 (2019).
5. K. L. McKinley, I. M. Cheeseman, *Nat. Rev. Mol. Cell Biol.* **17**, 16–29 (2016).
6. P. B. Talbert, S. Henikoff, *Exp. Cell Res.* **389**, 111895 (2020).
7. O. J. Marshall, A. C. Chueh, L. H. Wong, K. H. A. Choo, *Am. J. Hum. Genet.* **82**, 261–282 (2008).
8. K. F. Sullivan, M. Hechenberger, K. Masri, *J. Cell Biol.* **127**, 581–592 (1994).
9. K. Yoda *et al.*, *Proc. Natl. Acad. Sci. U.S.A.* **97**, 7266–7271 (2000).
10. D. Fachinetti *et al.*, *Nat. Cell Biol.* **15**, 1056–1066 (2013).
11. E. M. Dunleavy, G. Almouzni, G. H. Karpen, *Nucleus* **2**, 146–157 (2011).
12. D. L. Bodor, L. P. Valente, J. F. Mata, B. E. Black, L. E. T. Jansen, *Mol. Biol. Cell* **24**, 923–932 (2013).
13. L. E. T. Jansen, B. E. Black, D. R. Foltz, D. W. Cleveland, *J. Cell Biol.* **176**, 795–805 (2007).
14. M. Schuh, C. F. Lehner, S. Heidmann, *Curr. Biol.* **17**, 237–243 (2007).
15. E. M. Dunleavy *et al.*, *Cell* **137**, 485–497 (2009).
16. D. R. Foltz *et al.*, *Cell* **137**, 472–484 (2009).
17. D. Pan *et al.*, *eLife* **6**, e23352 (2017).
18. Y. Fujita *et al.*, *Dev. Cell* **12**, 17–30 (2007).
19. F. Spiller *et al.*, *EMBO Rep.* **18**, 894–905 (2017).
20. R. Thamkachy *et al.*, Structural basis for Mis18 complex assembly: Implications for centromere maintenance. bioRxiv 466737 [Preprint] (2023); https://doi.org/10.1101/2021.11.08.466737.
21. I. K. Nardi, E. Zasadzińska, M. E. Stellfox, C. M. Knippler, D. R. Foltz, *Mol. Cell* **61**, 774–787 (2016).
22. M. E. Stellfox, I. K. Nardi, C. M. Knippler, D. R. Foltz, *Cell Rep.* **15**, 2127–2135 (2016).
23. D. Pan *et al.*, *Nat. Commun.* **10**, 4046 (2019).
24. J. Wang *et al.*, *J. Biol.* (2014).
25. G. Mizuguchi *et al.*, *Science* **303**, 343–348 (2004).
26. D. R. Foltz *et al.*, *Nat. Cell Biol.* **8**, 458–469 (2006).
27. J. Walfridsson *et al.*, *Nucleic Acids Res.* **33**, 2868–2879 (2005).
28. H. Izuta *et al.*, *Genes Cells* **11**, 673–684 (2006).
29. M. Perpelescu, N. Nozaki, C. Obuse, H. Yang, K. Yoda, *J. Cell Biol.* **185**, 397–407 (2009).
30. M. C. Barnhart-Dailey, P. Trivedi, P. T. Stukenberg, D. R. Foltz, *Mol. Biol. Cell* **28**, 54–64 (2017).
31. M. Okada, K. Okawa, T. Isobe, T. Fukagawa, *Mol. Biol. Cell* **20**, 3986–3995 (2009).
32. S. Müller *et al.*, *Cell Rep.* **8**, 190–203 (2014).
33. M. C. C. Silva *et al.*, *Dev. Cell* **22**, 52–63 (2012).
34. A. Stankovic *et al.*, *Mol. Cell* **65**, 231–246 (2017).
35. K. L. McKinley, I. M. Cheeseman, *Cell* **158**, 397–411 (2014).
36. M. Petronczki, P. Lénárt, J.-M. Peters, *Dev. Cell* **14**, 646–659 (2008).
37. V. Archambault, D. M. Glover, *Nat. Rev. Mol. Cell Biol.* **10**, 265–275 (2009).
38. G. Combes, I. Alharbi, L. G. Braga, S. Elowe, *Oncogene* **36**, 4819–4827 (2017).
39. S. Zitouni, C. Nabais, S. C. Jana, A. Guerrero, M. Bettencourt-Dias, *Nat. Rev. Mol. Cell Biol.* **15**, 433–452 (2014).
40. A. E. H. Elia *et al.*, *Cell* **115**, 83–95 (2003).
41. P. Singh *et al.*, *Mol. Cell* **81**, 67–87.e9 (2021).
42. J. Jumper *et al.*, *Nature* **596**, 583–589 (2021).
43. A. E. H. Elia, L. C. Cantley, M. B. Yaffe, *Science* **299**, 1228–1231 (2003).
44. P. J. Huis in 't Veld *et al.*, *eLife* **5**, e21007 (2016).
45. K. Suzuki *et al.*, *Sci. Rep.* **5**, 7929 (2015).
46. A. al-Rawi, E. Kaye, S. Korolchuk, J. A. Endicott, T. Ly, *Cell Rep.* **42**, 112139 (2023).
47. J. Holder, E. Poser, F. A. Barr, *FEBS Lett.* **593**, 2908–2924 (2019).
48. P. Parashara *et al.*, *Science* **385**, 1098–1104 (2024).

ACKNOWLEDGMENTS

We thank all the members of the Musacchio group for the helpful scientific discussions; R. G. Schönenbrücher and P. Geue (MPI Dortmund, Biophysics Facility) for support with SEC–multi-angle light scattering; P. Keller (MPI Dresden, Antibody Facility) for helping with antibody generation; C. Körner, A. Dammers, L. Schulze, and L. Oberste-Lehn for assisting with reagent preparation; N. Schmidt for support with image analysis; S. Maffini and J. Schweighofer for critical reading of the manuscript; and A. A. Jeyaprakash, P. Parashara, B. Medina-Pritchard, and M. A. Abad for sharing unpublished results and for discussions during the development of this study. **Funding:** This work was supported by the Max Planck Society (A.M.), the European Research Council (synergy grant 951430 BIOMECANET to A.M.), the Marie-Curie Training Network (DivIDE project number 675737 to A.M.), the German Research Foundation (DGF Collaborative Research Centre grant 1430 "Molecular Mechanisms of Cell State Transitions" to A.M.), the CANTAR network under the Netzwerke-NRW program (A.M.), and the European Molecular Biology Organization (EMBO long-term fellowship ALFT439-2019 to D.C.). **Author contributions:** Conceptualization: A.M., D.C.; Funding acquisition: A.M.; Investigation: D.C., A.E.V., I.R.V., D.P., V.C., M.E.P.; Methodology: D.C., A.E.V.; Project administration: A.M., D.C.; Supervision: A.M.; Visualization: D.C.; Writing – original draft: D.C.; Writing – review & editing: A.M., D.C., A.E.V., I.R.V. **Competing interests:** The authors declare no competing interests. **Data and materials availability:** All data are available in the main text or the supplementary materials. All cell lines and plasmids are available upon request.

SUPPLEMENTARY MATERIALS

science.org/doi/10.1126/science.ado5178
Materials and Methods
Supplementary Text
Figs. S1 to S22
Tables S1 to S5
References (*49*–*59*)
MDAR Reproducibility Checklist

Submitted 23 February 2024; accepted 30 July 2024
10.1126/science.ado5178